QM/MM molecular dynamics simulations of the hydration of Mg(II) and Zn(II) ions

Article *in* Canadian Journal of Chemistry · July 2013

DOI: 10.1139/cjc-2012-0515

3 authors, including:

Benoît Roux
The University of Chicago Medical Center
270 PUBLICATIONS **15,672** CITATIONS
SEE PROFILE

Christopher Rowley
Memorial University of Newfoundland
46 PUBLICATIONS **1,225** CITATIONS
SEE PROFILE

QM/MM Molecular Dynamics Simulations of the Hydration of Mg(II) and Zn(II) Ions

Saleh Riahi, Benoît Roux, and Christopher N. Rowley

Abstract: The hydration of Mg^{2+} and Zn^{2+} is examined using molecular dynamics simulations using three computational approaches of increasing complexity: the CHARMM non-polarizable force field based on the TIP3P water model, the Drude polarizable force field based on the SWM4-NDP water model, and a combined QM/MM approach in which the inner coordination sphere is represented using a high quality density functional theory (DFT) model (PBE/def2-TZVPP) and the remainder of the bulk water solvent is represented using the polarizable SWM4-NDP water model. The characteristic structural distribution functions (radial, angular, and tilt) are compared, which show very good agreement between the polarizable force field and QM/MM approaches. They predict an average Mg–O distance of 2.11 Å and an Zn–O distance of 2.13 Å, in good agreement with the available experimental neutron scattering and EXAFS data, while the Mg–O distances calculated using the non-polarizable force field are 0.1 Å too short. Mg^{2+}(aq) and Zn^{2+}(aq) both have a coordination number of 6 and have a remarkably similar octahedral coordination mode, despite the chemical differences between these ions. Thermodynamic integration was used to calculate the relative hydration free energies of these ions ($\Delta\Delta G_{\mathrm{hydr}}$). The non-polarizable model is in error by 60 kcal mol^{-1} and incorrectly predicts that Mg^{2+} has the more negative hydration energy. The Drude polarizable model predicts a $\Delta\Delta G_{\mathrm{hydr}}$ of only –13.2 kcal mol^{-1}, an improvement over the results of the non-polarizable force field, but still signficantly different than the experimental value of –30.1 kcal mol^{-1}. The combined QM/MM approach performs much better, predicting a $\Delta\Delta G_{\mathrm{hydr}}$ of –34.8 kcal mol^{-1} in excellent agreement with experiment. These calculations support the experimental observation that Zn^{2+} has more favourable solvation free energy than Mg^{2+} despite having a very similar solvation structure.

Key words: ion solvation, Mg^{2+}, Zn^{2+}, molecular dynamics, polarizable force fields, QM/MM, thermodynamic integration.

Résumé : L'hydratation des ions divalent Mg^{2+} and Zn^{2+} est étudiée à partir de simulations de dynamique moleculaire et trois approches théoriques de complexité croissante : le champ de force non-polarisable de CHARMM basé sur le modèle de molécules d'eau TIP3P, le champ de force polarisable Drude basé sur le modèle de molécules d'eau SWM4-NDP, et une approche QM/MM pour laquelle la sphere de coordination est representée par une méthode *ab initio* de haute précision basée sur la théorie de fonctionelle de densité (PBE/def2-TZVPP) tandis que les molécules d'eau plus distantes sont décrites part le modèle polarisable SWM4-NDP. Les propriétées structurales ainsi que les fonctions de distribution (radiale, angulaire et azimutale) sont calculées et comparees, démontrant un excellent accord entre le champ de force polarisable et l'approche QM/MM. La distance Mg–O moyenne au contact est de 2.11 Å et la distance Zn–O moyenne est de 2.13 Å. Ces résultats sont en excellent accord avec les donnees expérimentales obetenu par diffusion des neutrons et EXAFS. La distance Mg–O moyenne au contact obtenue par le champ de force non-polarisable est trop courte de 0.1 Å$\dot{\mathrm{M}}g^{2+}$ et Zn^{2+} ont tous deux un nombre de coordination de 6 et ont un mode de coordination octaédrique remarquablement similaires, malgré les différences chimiques entre ces ions et le grande différence d'énergie libre d'hydration entre ces deux ions ($\Delta\Delta G_{\mathrm{hydr}}$). Un calcul d'intégration thermodynamique permet d'estimer $\Delta\Delta G_{\mathrm{hydr}}$ et de comparer avec la valeur experimentale de –30.1 kcal mol^{-1}. Le modèle non-polarisable prédit incorrectement que l'ion Mg^{2+} est plus fortement hydrate que Zn^{2+} avec une erreur d'environ 60 kcal mol^{-1}. Un meilleur résultat est obtenu avec le modèle Drude polarisable, mais le $\Delta\Delta G_{\mathrm{hydr}}$ est sous-estimé à –13.2 kcal mol^{-1}. Enfin, un $\Delta\Delta G_{\mathrm{hydr}}$ de –34.8 kcal mol^{-1} est obtenu avec l'approche QM/MM, en excellent accord avec la valeur experimentale. Ces calculs démontrent que l'ion Zn^{2+} est plus favorablement hydraté que l'ion Mg^{2+} bien que ces deux ions possèdent une structure d'hydration très semblable.

1. Introduction

The solvation of ions is an enduring fascination of physical, inorganic, and analytical chemists. The interaction between an ion and the solvent is strongly dependent on the properties of the ion, such as its size, valency, polarizability, and Lewis acidity/basicity.[1;2] These interactions ultimately affect the macroscopic physical properties of the solution in the form of colligative properties, electrokinetic phenomena, and electrical conductivity.

The hydration of the divalent ions Mg^{2+} and Zn^{2+} have particularly interesting parallels. Although Mg^{2+} is an alkaline earth metal and Zn^{2+} is a d^{10} transition metal, they have very similar ionic radii (0.72 Å and 0.74 Å, respectively).[3] The Born model of ion solvation predicts that two ions of the same valency and radii should have the same solvation free energies, however the reported free energy of solvation of Zn^{2+} is approximately 30 kcal mol^{-1} more negative than that of Mg^{2+}.[4] This suggests that difference between these ions stems from more subtle effects.

As the molecular level interactions between an ion and its solvent are difficult to study experimentally, molecular dynamics simulations are frequently used to examine the structure and dynamics of solvated ions. These simulations typically

employ computationally efficient molecular mechanical (MM) models so that the full complexity of the ion and its environment can be represented. Small, divalent ions like Mg^{2+} and Zn^{2+} pose serious challenges for conventional molecular mechanical force fields because the ion–ligand distances are exceptionally short (e.g. $r_{M-O} \approx 2$ Å in water). At these distances, the divalent charge of these ions will strongly polarize the coordinating water molecules, so a conventional non-polarizable MM force field will not accurately describe this interaction. To address this issue, parameters for the interaction of Mg^{2+} and Zn^{2+} with water have been determined for both the AMOEBA[5;6] and Drude force fields,[7] which include terms to allow for the effects of induced electron polarization. These models show improved ion–water interaction energies and free energies of hydration.

Although polarizable force fields are capable of approximating the effects of induced polarization, several additional parameters must be defined based on limited experimental or quantum mechanical target data. As a result, it is not clear how accurately these models describe the structural features of the ionic solvation structure. Further, the absolute ion solvation free energies used to parameterize and validate these models are difficult to ascertain experimentally, introducing a degree of error. Experimental techniques for characterizing ion-water structure, such as neutron diffraction or X-ray scattering, provide only coarse structural features, so these models cannot be thoroughly validated by experimental data alone.

Ab initio molecular dynamics (AIMD) is an alternative strategy to examine the structure and thermodynamics of solvated ions. By performing a molecular dynamics simulation using a quantum mechanical (QM) representation of the ion and solvent, these methods can sample the configurational space of a solvated ion without the definition of force field parameters. Electron polarization and charge transfer effects are inherently included in these models. The downside of these QM models is that they are much more computationally expensive than MM models, so the number of solvent molecules that can be included is more limited and simulation time scales are much shorter. Further, these QM models are also inexact due to approximations in the density functional theory (DFT) exchange-correlation functionals, pseudopotential representations, and truncation of the basis set. These limitations can affect the calculated ion solvation structure, so previous reports based on AIMD simulations of Mg^{2+} and Zn^{2+} have a range of conclusions.[8;9;10;11;12;13;14;15] Hybrid QM/MM simulations are an obvious means to perform ab initio simulations of ion solvation at a reduced computational cost. There is a natural division of QM and MM regions, as the ion and the solvent molecules nearest to it can be represented using the QM methods while rest of the solvent can be represented using the MM model. We employed this strategy in a recent study where high level QM/MM molecular dynamics simulations were used to model the solvation of Na^+ and K^+ in liquid water.[16] We attempted to limit the approximations in this model by using a large all-electron triple-ζ basis set and embedding the ion and nearest water molecules in a 14 Å sphere of polarizable MM water molecules.

The hydration of Mg^{2+} and Zn^{2+} are ideal subjects for this kind of study, as complex electronic effects are important in these ions and they have a small inner coordination sphere. In particular, an accurate first-principles description of their characteristic structural distribution functions, with a consistent computational methodology would establish how similar the solvation structure of these ions is. Additionally, calculating the relative solvation free energy of these ions using thermodynamic integration would test the surprising experimental result that Zn^{2+} has a more negative solvation free energy than Mg^{2+}. In this paper, we report extended QM/MM molecular dynamics simulations on Mg^{2+}(aq) and Zn^{2+}(aq). The QM system was described using DFT and a large basis set, embedded in an MM sphere of Drude polarizable water molecules. These models are compared to the results from the CHARMM non-polarizable and Drude polarizable force fields.

2. Computational Methods

All MM calculations were performed using CHARMM[17] version c37b2. QM/MM calculations were performed using CHARMM c37b2 interfaced with TURBOMOLE 6.3[18] through the QTURBO module. The equations of motion were propagated using the velocity Verlet algorithm,[19] modified by a Langevin thermostat to sample the canonical ensemble of configuration at a temperature of 298.15 K. For systems containing Drude particles, a dual Langevin thermostat was applied, where the first thermostat maintained the temperature of the atomic centers at 298.15 K and the second thermostat maintained the temperature of the Drude particles at 1 K. The ion was restrained at the center of a sphere of 451 water molecules with a radius of 14 Å. The water molecules were confined to this sphere by a half-cubic restraining function. All water molecules were constrained to their equilibrium liquid-phase bond lengths and angles using the SHAKE algorithm.[20] A 1 fs time step was used in all simulations.

The non-polarizable models used the TIP3P model for water[21] and standard CHARMM force field parameters for Mg^{2+} and Zn^{2+}. The Lennard-Jones parameters for these ions were $E_{\min} = 0.015$ kcal mol^{-1} $R_{\min} = 2.37$ Å for Mg^{2+} and $E_{\min} = 0.25$ kcal mol^{-1} $R_{\min} = 2.18$ Å for Zn^{2+}. The Drude polarizable models used the SWM4-NDP model for water[22] and the ionic parameters of Yu et al.[7] The non-polarizable and Drude MM models were equilibrated for 1 ns followed by a production run of 4 ns.

The QM/MM calculations employed the same sphere of water molecules as the MM models. The QM region included the ion and the six nearest water molecules. All the remaining water molecules were represented using the SWM4-NDP Drude polarizable water model.[22] SWM4-NDP is an accurate model

Saleh Riahi. Department of Chemistry, Memorial University of Newfoundland, St. John's, Newfoundland, Canada A1B 3X7
Benoît Roux.[1] Department of Biochemistry and Molecular Biology, The University of Chicago, 929 East 57th Street, Chicago, Illinois, United States
Christopher N. Rowley.[2] Department of Chemistry, Memorial University of Newfoundland, St. John's, Newfoundland, Canada A1B 3X7

[1]Corresponding author (e-mail: roux@uchicago.edu).
[2]Corresponding author (e-mail: cnrowley@mun.ca).

for the mechanical, transport, and thermodynamic properties of bulk water. In particular, the static dielectric constant of SWM4-NDP water is consistent with the experimental value of $\epsilon = 78$, whereas many non-polarizable models significantly overestimate the dielectric constant.

A QM region of six waters was chosen because previous reports found both Mg^{2+} and Zn^{2+} to have inner coordination spheres that are consistently hexacoordinate. An earlier QM/MM study of Zn^{2+}(aq) by Cauet et al.[13] found that there was no advantage to using a QM region larger than six water molecules. A report by Callahan et al. showed that $MgCl_2$ solutions do not form contact ion pairs even at very high concentrations, so we have focused on the infinitely dilute case of a single solvated dication.[23] This small QM region allows us to use a larger basis set and perform longer simulations. The QM region was represented using DFT with the PBE exchange-correlation functional.[24] This functional was chosen as it is non-empirical and has performed well across a wide range of chemical systems. As this is a pure functional and no exchange integrals were needed,it was possible to employ the highly efficient resolution of identity (RI) approximation.[25] The triple-ζ def2-TZVPP basis set was assigned for all atoms to limit basis set truncation and basis set superposition error.[26] An SCF convergence criteria of 10^{-7} was imposed to ensure accurate energies and gradients and the m5 grid was used for integration in the exchange-correlation term. The effect of the MM point charges to the QM region was calculated by including the one-electron integrals between the MM point charges and the QM basis functions in the Fock matrix. Lennard-Jones interactions between the QM and MM waters were adjusted to recreate the QM dimerization energies, as described in Ref. 16. Although we have developed an effective and rigorous method to prevent exchange of QM and MM water molecules from the solvent,[16] it was not necessary to use this method in this case because no such exchanges occurred during the time scale of our QM/MM simulations. These QM/MM models were equilibrated for 2 ps followed by a 98 ps production run. Although shorter simulations have been used in previous AIMD simulations, we performed these longer simulations to ensure the distributions were sampled sufficiently.

2.1. Thermodynamic Integration

The difference in solvation free energies of Mg^{2+}(aq) and Zn^{2+}(aq) was calculated using alchemical thermodynamic integration, using a linear interpolation between the Mg^{2+}(aq) and Zn^{2+}(aq) states. 11 simulations were performed at values of λ between 0.0 and 1.0 separated by increments of 0.1. For the MM models, each value of λ was equilibrated for 400 ps followed by a 1 ns production period.

$$[1] \qquad \Delta G_{Mg^{2+}(aq)\rightarrow Zn^{2+}(aq)} = \int_{\lambda=0}^{\lambda=1} \langle U_{Zn} - U_{Mg} \rangle_{\lambda} \, \mathrm{d}\lambda$$

The QM/MM relative solvation free energies were calculated using an analogous thermodynamic integration procedure, where the path between the QM/MM Mg^{2+} system ($\lambda = 0$) and QM/MM Zn^{2+} ($\lambda = 1$) system was calculated by interpolating between the two QM/MM Hamiltonians. The difference in electronic energy of the bare Mg^{2+} and Zn^{2+} ions was calculated separately and subtracted from the energy differences. This method is described in detail in an excellent review by Salahub and coworkers.[27] For each value of λ, the system was equilibrated for 2 ps before a 15 ps production period.

The free energy differences of each system were calculated from the time series of our free energy perturbation (FEP) simulations data using the WHAM.[28] The intrinsic solvation free energies were were corrected for the phase potential of the water models using the water model interfacial potentials determined in Ref. 29.

2.2. Absolute Solvation Free Energies

The absolute solvation free energies for the non-polarizable and Drude MM models were calculated using FEP/MD simulations by decoupling a single ion from a solvent of 450 ($24\ \mathring{A} \times 24\ \mathring{A} \times 24\ \mathring{A}$) water molecules under periodic boundary conditions. For electrostatic interactions, particle mesh Ewald (PME) scheme with $\kappa = 0.33$ and sixth order spline function was applied. Lennard-Jones and the real space electrostatic nonbonded interactions were calculated using a switching function between distances of 10 Å and 12 ÅFor each window, a 400 ps equilibriation simulation was performed, followed a 1 ns sampling period, with a time step of 1 fs. These simulations were performed using isothermal–isobaric molecular dynamics, with a Nosé–Hoover thermostat.[30] In the case of the Drude polarizable model, a dual thermostat was used, where the first thermostat at $T = 298.15$ K was coupled to the heavy atoms with a relaxation time of 0.1 ps and the second thermostat at $T^* = 1$ K with was coupled to the Drude particles with a relaxation time of 0.005 ps for the Drude particles. Fictious masses of 0.4 amu were assigned to the Drude particles. The Andersen–Hoover barostat[31] with a relaxation time of 0.2 ps was used to maintain a pressure of a 1 atm.

In order to calculate absolute energy of hydration of Mg^{2+} and Zn^{2+}, we used the decoupling methodology of Deng and Roux.[32] In this technique, the absolute hydration free energy the ion $\Delta_{hydr}G$ is calculated as the sum of three contributions corresponding to the electrostatic, dispersive, and repulsive interactions between the ion and solvent,

$$[2] \qquad \Delta_{hydr}G = \Delta G_{elec} + \Delta G_{disp} + \Delta G_{rep}$$

The electrostatic component (ΔG_{elec}) was calculated using thermodynamic integration of a path where the charge of the ion was reduced to zero through the coupling parameters λ. This path was calculated over 11 values of λ in increments of 0.1 between 0 and 1. An analogous FEP path as used to calculate the dispersion component of the Lennard-Jones interaction (ΔG_{disp}) using the Weeks–Chandler–Andersen decomposition. For the repulsive component (ΔG_{rep}), the staging parameter, s, was used to calculate the free energy change at values of 0.0, 0.2, 0.3, 0.4, 0.5, 0.6, 0.7, 0.8, 0.9, and 1.0. For each value of s, simulations were performed at $\lambda = 0$ and $\lambda = 1$. Using the time series of the FEP data from these simulations, ΔG_{elec} was calculated using trapezoidal rule, while ΔG_{disp} and ΔG_{rep} were calculated using WHAM.[28]

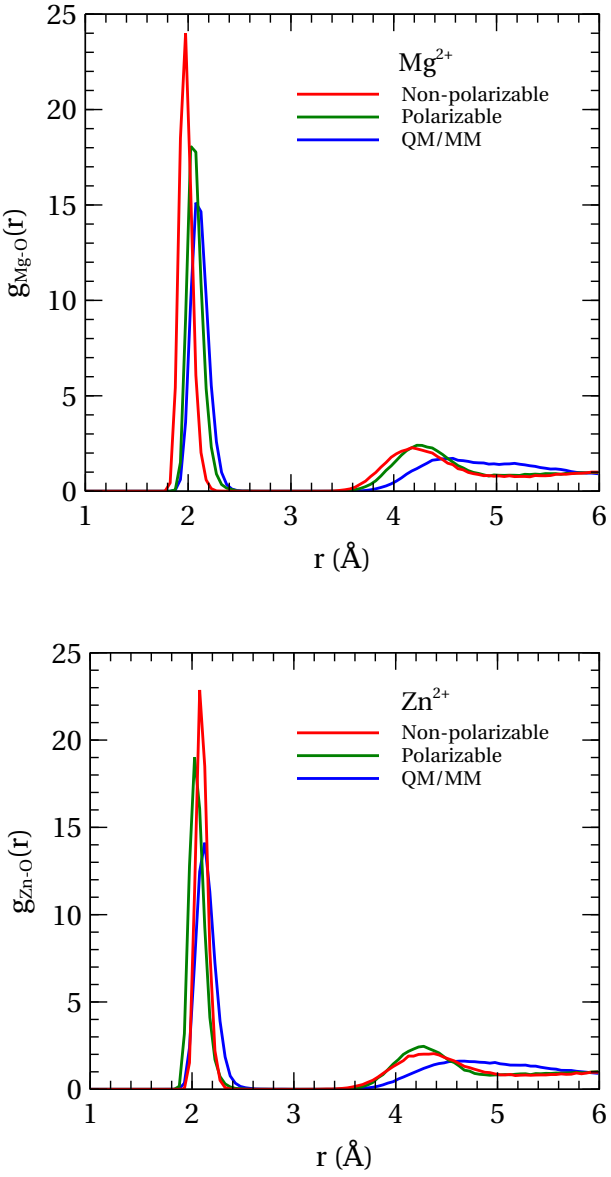

Fig. 1. M–O radial distribution functions calculated from MD simulations with the CHARMM non-polarizable force field, Drude polarizable force field, and combined QM/MM approach.

Table 1. Binding energy and M–O distance of $M(OH_2)_6^{2+}$.

Model	ΔE_{Mg} b (kcal mol^{-1})	Mg–O (Å)	ΔE_{Zn} (kcal mol^{-1})	Zn–O (Å)
Non-polarizable	–340.1	1.98	–310.8	2.10
Drude	–323.1	2.08	–334.6	2.06
PBE/def2-TZVPP	–325.3	2.11	–356.5	2.13

3. Results and Discussion

3.1. Ion Solvation Structure

3.1.1. Radial Distribution Functions and Coordination Numbers

The ion–O radial distribution function (RDF, $g(r)$) is a correlation function that relates the density of the solvent at a distance, r, from the ion, to the bulk density. Values less than one indicate a depletion of solvent density, while values greater than one indicate an increase. The location of the first coordination sphere of an ion is easily identifiable from the RDF, as there is a sharp peak at this distance. The RDFs calculated from our molecular dynamics simulations are presented in Fig. 1.

Table 2. Ion–O distances for Mg^{2+}(aq) and Zn^{2+}(aq). Values from computer simulations are taken as radius where the maximum of the M–O RDF occurs.

Method	Mg–O (Å)	Zn–O (Å)
Non-polarizable	1.98	2.09
Drude	2.05	2.03
QM/MM	2.11	2.13
AMOEBA	2.07[5]	1.98[6]
AMOEBA-VB	-	2.06[33]
Previous AIMD	2.10[8]	2.18[13]
	2.13[9]	2.18[14]
	2.08[10]	2.09[15]
	2.08[11]	
	2.13[12]	
exptl.	2.10[34]	2.08[35]

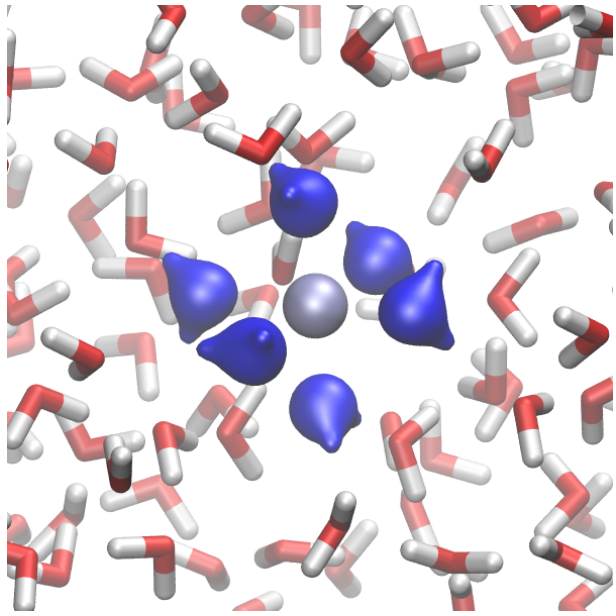

Fig. 2. Representative configuration of QM/MM model of Mg^{2+}(aq). The electron density distribution for the QM region is shown in blue. The Mg^{2+} ion is shown in light blue.

The RDFs of Mg^{2+}(aq) are in generally good agreement, with a sharp peak for the first coordination sphere near 2.1 Å. This distance is consistent with neutron diffraction data that gives a Mg–O distance of 2.10 Å[34] and with most previous AIMD simulations (Table 2).[3] These distances are close to those calculated from the optimized structure of $Mg^{2+}(OH_2)_6$ (Table 1), which shows that the inner coordination sphere remains near its gas phase potential energy minimum. The integral of this peak over spherical coordinations gives a coordi-

[3] The neutron diffraction data was collected from 0.2 M $MgCl_2$. Callahan et al.[23] determined that ion pairing is not significant at these concentrations.

nation number of 6.0, indicating that the ion maintains a constant coordination number of 6 throughout the simulation. A representative configuration from the QM/MM simulation of Mg^{2+}(aq) that illustrates this inner sphere is presented in Fig. 2.

The non-polarizable force field predicts the Mg^{2+}–O distance to be slightly shorter than the other methods, with a maximum near 2.0 Å. In contrast to alkali cations, there is a sharp separation between the first coordination sphere and the rest of the solvent; the RDF has a value of zero until the second coordination sphere that occurs near $r = 4.0$ Å. The RDFs calculated from the QM/MM and Drude simulations are in very good agreement, although the first peak of the Drude RDF is higher and more narrow the the QM/MM model. This reflects that the MM models use a Lennard-Jones potential to represent repulsive interactions, which is a harder repulsive force than Pauli repulsion forces are in reality.

The RDFs of Zn^{2+}(aq) show quite similar trends. In this case, all models predict a sharp peak for the first coordination sphere with centers that range between 2.09–2.13 Å. This distance is consistent with the experimental EXAFS and XANES spectra that indicate an average Zn^{2+}–O distance of 2.08 Å.[35;36] [4] Our simulations are in better agreement with the experimental value than some other AIMD simulations, which predict larger Zn^{2+}–O distances (Table 2). The Zn^{2+}–O distance appears to be sensitive to the QM method and basis set. Our use of an all electron triple-ζ basis set may explain the improved accuracy of our simulations. As for the Mg^{2+}(aq) RDF, the non-polarizable MM model predicts a sharper first peak than the other methods and the QM/MM has the broadest peak, reflecting a broader range of accessible configurations. The spherical integral of the Zn^{2+}–O radial distribution function is exactly 6.0 for all these methods, indicating that Zn^{2+} is also consistently predicted to be six coordinate.

3.1.2. Angular Distribution Functions

The angular distribution function (ADF) is the probability distribution of the angles formed between the oxygen atoms of inner-sphere water molecules and the ion. High probabilities of finding water molecules trans to each other ($\theta = 180°$, $\cos\theta = -1$) and cis to each other ($\theta = 90°$, $\cos\theta = 0$) are indicative of an octahedral coordination mode. The ADFs calculated from our molecular dynamics simulations are presented in Fig. 3.

For Mg^{2+}, the ADF of all methods show narrow, discrete distributions centered at $\cos\theta = -1$ and $\cos\theta = 0$. This indicates that at 298.15 K, Mg^{2+} makes only moderate oscillations around an octahedral coordination structure. The CHARMM and Drude MM models are in close agreement, with very sharp peaks in the distribution functions, although the QM/MM distribution is broader. These broader distributions can be explained by the rigorous treatment of electron polarization in the QM/MM model, which can stabilize configurations with more acute O–M–O angles. The approximate treatment of polarizability in the Drude model is not able to reproduce this effect fully.

The ADFs of Zn^{2+} show greater variety. The QM/MM distribution very similar to that of QM/MM simulation for Mg^{2+}(aq), holding a fairly narrow six-coordinate octahedral orientation. The MM models yield more narrow distributions, although in contrast to the distributions for Mg^{2+}(aq), the simulation with the Drude model produces a more narrow distribution than the non-polarizable model. The use of a large Thole screening coefficient to correct for overpolarization in the Zn^{2+}–OH_2 interaction may account for this difference.

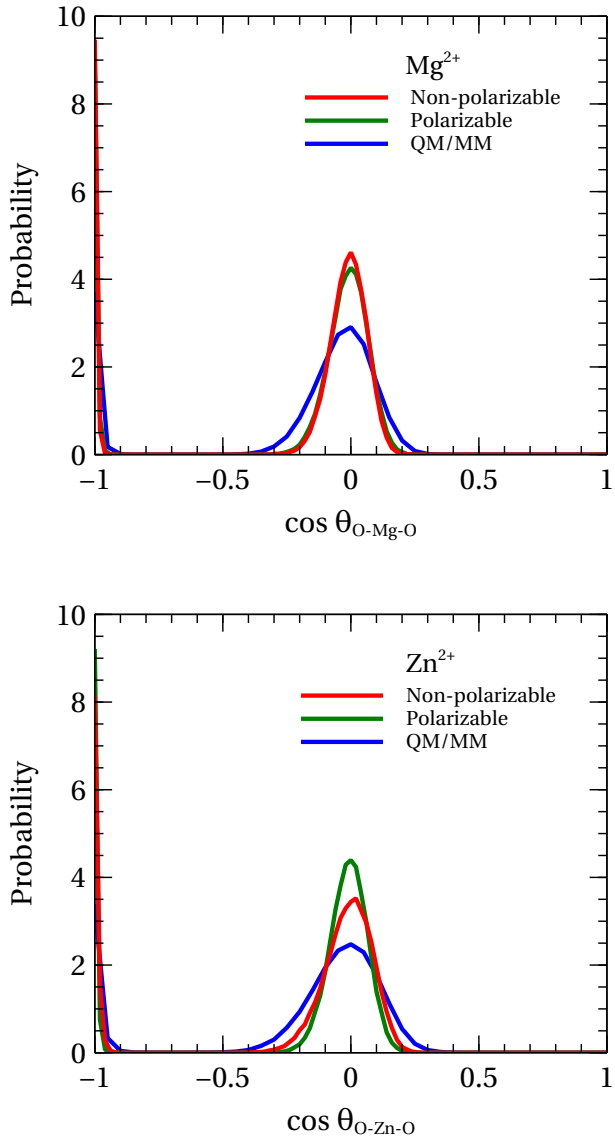

Fig. 3. Water–ion–water angle distribution functions for waters in the first coordination sphere ($r_{M-O} < 2.5$ Å).

3.1.3. Tilt Distribution Function

The tilt distribution function shows the distribution of the angle (φ) formed between the ion, the oxygen atom of the inner sphere water molecules, and the bisector of the O–H bonds. When $\cos\varphi$ is equal to -1, the axis of the water molecule is aligned with the ion. This distribution is a measure of the strength of the ion-water charge-dipole interaction, which is strongest when the dipole moment of the water is aligned with ionic charge. The tilt distribution functions calculated from our molecular dynamics simulations are presented in Fig. 4.

The tilt distributions of the Drude and QM/MM simulations of Mg^{2+}(aq) are in reasonably good agreement, with distribu-

[4] EXAFS measurements in Ref. 35 were made of 0.2 M solutions of $ZnNO_3$, where ion pairing effects are not likely to be signficant.

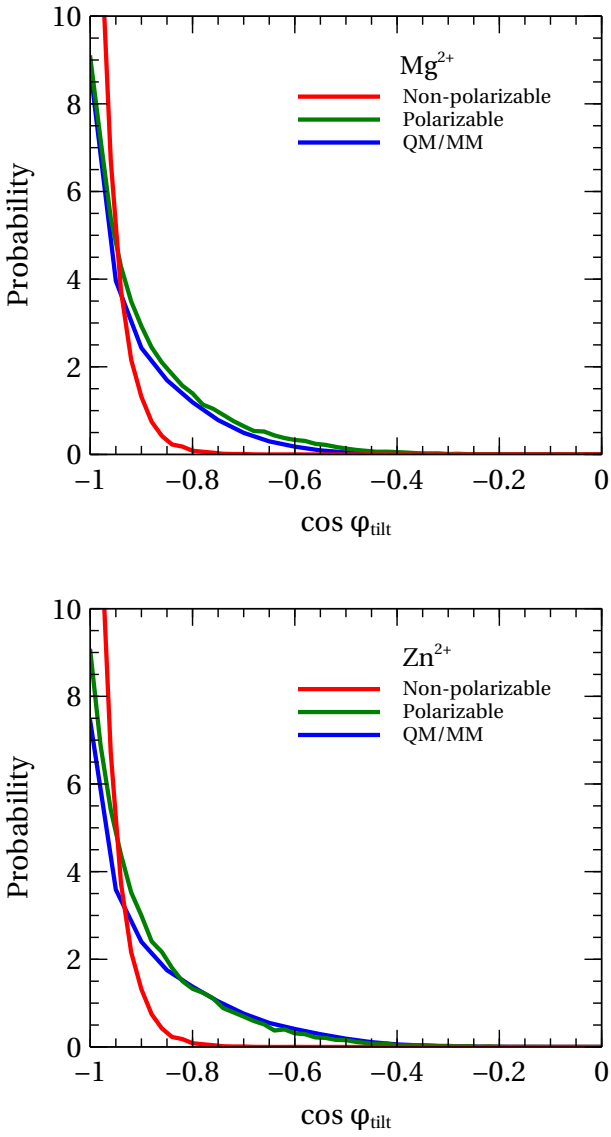

Fig. 4. Tilt angle distributions (ion–O–H bisector) for waters in the first coordination sphere ($r_{M-O} < 2.5$ Å).

tions that are peaked at $\cos\varphi = -1$ ($\varphi = 180°$) and decay to a low probability near $\cos\varphi = -0.5$ ($\varphi = 135°$), although the QM/MM distribution is slightly broader. The non-polarizable CHARMM MM distribution is sharpest, with the distribution decaying to zero near $\cos\varphi = -0.25$ ($\varphi = 104°$). This reflects the high permanent dipole of the TIP3P water model ($\mu_\circ = 2.347$ D) and the lack of induced electron polarization in this model.

The tilt distributions of Zn^{2+}(aq) show very similar trends and are generally very similar to the tilt distributions for Mg^{2+}(aq). This suggests that the tilt distributions of these ions is primarily dependent on the size and valency of the ions and the description of electron polarization in the coordinating water molecules.

3.2. Solvation Free Energies

Absolute ion solvation free energies are difficult to calculate because the large change in free energy necessitates very long simulation times to achieve sampling to convergence. Relative solvation free energies are more straightforward, as they can be determined using thermodynamic integration of an alchemical path between two similar states. These relative solvation free energies can also be compared readily to the experimental relative solvation energies of two neutral salts with the same anion (e.g. $MgCl_2$ and $ZnCl_2$), which can be determined accurately without extrathermodynamic assumptions. We used the thermodynamic integration technique to calculate the relative hydration free energies of Mg^{2+} and Zn^{2+} for the non-polarizable, Drude, and QM/MM models (Table 3).

Method	$\Delta\Delta G_{\mathrm{hydr}}$ (kcal mol^{-1})
CHARMM	31.1
Drude	–13.2
AMOEBA	–27.8
QM/MM	–34.8
exptl.[7]	–30.2

Table 3. Relative free energies of hydration of $Mg^{2+} \rightarrow Zn^{2+}$ ($\Delta\Delta G_{\mathrm{hydr}}$).

The $\Delta\Delta G_{\mathrm{hydr}}$ calculated using the QM/MM approach is in good agreement with experiment. This provides support for the experimental result that the relative solvation free energy of the two ions is roughly 30 kcal mol^{-1}. This difference is close to the relative potential energy of coordination for $Mg^{2+}(OH_2)_6$ and $Zn^{2+}(OH_2)_6$ (Table 1), suggesting that the difference in solvation free energies of the two ions is primarily due to stronger intermolecular interactions between the inner sphere water molecules and the ion, despite the ion–water distances being very similar. DFT calculations by Wu et al.[6] indicated that there is a significant ligand to metal charge transfer between coordinating water molecules and a Zn^{2+} ion, which could account for this difference.

The non-polarizable CHARMM models perform least effectively, resulting in a relative solvation free energy of +30 kcal mol^{-1}, an error of 60 kcal mol^{-1} and incorrectly predicting Mg^{2+} to have the more negative ion hydration energy of the two ions. This difference in energy can be correlated to the smaller size of the Mg^{2+} ion that is apparent in the radial distribution function, which leads to stronger ion–water interactions. It is unlikely that any conventional non-polarizable model could accurately predict both the relative size and hydration energies of these two ions, as the more negative solvation free energy of Zn^{2+} occurs despite Zn^{2+} being essentially the same size as Mg^{2+} is counter to the expectation of a simple electrostatic description.

The Drude polarizable model performs better than the non-polarizable model in the calculation of relative solvation free energies, but falls short of quantitative accuracy. The solvation free energy is calculated to be –13.8 kcal mol^{-1}, in error by –16.2 kcal mol^{-1} from the experimental result. This discrepancy could be explained by the neglect of ion-water charge transfer and limitations of the Drude model for polarization. It is possible that the parameters of the Drude model could be revised to predict the free energy difference more accurately, as the original fitting was performed to reproduce a limited set of experimental data.

In principle, the Lennard-Jones parameters of the non-polarizable

Table 4. Absolute solvation free energy hydration of Mg^{2+} and Zn^{2+} calculated molecular mechanical models.

Model	$\Delta_{hydr}G$ (kcal mol^{-1})	
	Mg^{2+}	Zn^{2+}
Non-polarizable	–407.7	–376.6
Drude	–450.2	–463.1
exptl. (est)	–435.4[1]	–467.7[2]

[1] Ref. 38
[2] Ref. 4

model could be adjusted to provide better agreement with experiment, although it is worth noting that classical arguments based on the Born model,

$$\Delta\Delta G_{\rm hydr} = \frac{1}{2}\frac{q_{\rm ion}^2}{R_{\rm ion}}\left(\frac{1}{\epsilon}-1\right) \quad [3]$$

would require a difference of about 0.25 Å in the radius of Mg^{2+} and Zn^{2+} to match the free energy difference of 30 kcal mol^{-1} that is observed experimentally. The effective Born radii $R_{\rm ion}$ entering Eq. 3 are indirectly related to the position of the first maximum in the radial distribution function of these ions.[37] According to the radial distribution of Mg^{2+} and Zn^{2+} the radii should differ by at most 0.03 Å, pointing to a glaring failure of a purely classical treatment in this case. This supports the notion that QM effects underlie the large free energy difference.

It is possible to calculate the absolute solvation free energies of molecular mechanical models using a decoupling method. The limitations of the non-polarizable model are more apparent when we compute the absolute solvation free energies of these ions, which is straightfoward for molecular mechanical models. Table 4 shows the absolute solvation free energies calculated using the non-polarizable and Drude polarizable models. Although it is impossible to determine absolute solvation free energies with experimentally without invoking extrathermdynamic assumptions, we can use the reported experimental values as rough guide to magnitude of the absolute solvation free energies. The Drude polarizable force field was parameterized to reproduce the solvation free energies of neutral salts and is in reasonable agreement with experimental estimates of the absolute solvation free energies. The non-polarizable models predict absolute solvation free energies that are lower than the experimental estimates by 27.7 kcal mol^{-1} and 91.1 kcal mol^{-1} for Mg^{2+} and Zn^{2+}, respectively. The non-polarizable force field performs relatively well for Mg^{2+}(aq) only because it underestimates the Mg–O distances, leading to stronger ion-water interactions. This underestimation of the absolute solvation free energies reflects the lack of induced polarization and charge transfer effects in the non-polarizable force field, an effect that is sizable in the solvation of these ions. The only way to produce more accurate solvation free energies with this model would be to decrease the radius of the ions to the point that the ion–water distances would be unrealistically small.

We can also compare to the solvation energies reported for the Mg^{2+} and Zn^{2+} ions parameterized for the AMOEBA polarizable force. Based on the difference of the reported absolute free energies for Mg^{2+} and Zn^{2+}, the relative solvation free energy of these two ions is –27.8 kcal mol^{-1}, which is close to the experimentally measured value of –30.0 kcal mol^{-1}. It should be noted that the AMOEBA model predicts the Zn–O distances to be roughly 0.1 Å smaller than the Mg–O distances. Neither the QM/MM or experimental scattering data support such a large difference in radii and instead predict Zn^{2+} to be slightly larger than Mg^{2+}. The Born model predicts that this 0.1 Å difference in radii would account for a –14.4 kcal mol^{-1} difference in the hydration free energy, so part of the success of the AMOEBA model may simply be because it underestimates the average Zn–O distance. The AMOEBA force field with Valence Bond terms (AMOEBA-VB) predicts more realistic Zn–O distances, although the hydration free energy for this model has not yet been reported.[33]

4. Conclusions

In this paper, we have calculated the radial, tilt, and angular distribution functions for the solvation of the Mg^{2+} and Zn^{2+} ions in liquid water using molecular dynamics simulations. We compare the non-polarizable CHARMM force field, the Drude polarizable force field, and a QM/MM model. Our simulations confirm the established view that both these ions have a hexacoordinate inner coordination sphere with an octahedral structure. The inner coordination sphere is highly ordered and is separated from the bulk solvent. The non-polarizable force field provides reasonable radial structures and coordination numbers of the two ions, although they do not correctly describe the relative differences of the two ions and overestimate the ion water coordination energies. The Drude MM model shows good agreement with the QM/MM model for ion–O distances and coordination energies in comparison to the non-polarizable model.

The relative solvation free energies of these ions were calculated using thermodynamic integration for the non-polarizable, Drude, and QM/MM methods. The non-polarizable MM method is in error by a significant amount and incorrectly predicts Mg^{2+} to have the more negative solvation free energy. The Drude MM force field underestimates the relative solvation free energy by –17 kcal mol^{-1}. The QM/MM method is most accurate, predicting the relative free energy within 5 kcal mol^{-1} of the experimental value. The QM/MM relative solvation free energy confirms the surprising inference from experimental data that Zn^{2+} has a significantly more negative hydration free energy in comparison to Mg^{2+} despite having the same net charge and a generally similar solvent structure. The implication is that the large free energy difference arises from some non-classical QM component that is not present in MM models, even in a polarizable model.

The QM/MM model used in this study is very effective for modeling the structures and thermodynamics of Mg^{2+} and Zn^{2+} ions in liquid water, as it is in good agreement with both the structural and thermodynamic experimental data. This method has potential to be a valuable tool for understanding the Mg^{2+} vs Zn^{2+} selectivity of binding sites in biomolecules such as proteins, nucleic acids, and phospholipids.

5. Acknowledgements

CNR and SR thank the Memorial University of Newfoundland, NSERC of Canada for funding through a Discovery Grant

(Application No. 418505-2012), and the Research and Development Corporation of Newfoundland for an Ignite R&D grant. Computational resources were provided by the Extreme Science and Engineering Discovery Environment (XSEDE) supported by National Science Foundation grant number OCI-1053575, the Computation Institute of the University of Chicago, the Argonne National Lab, and the Compute Canada SciNet and ACEnet consortia. This work was supported by the National Science Foundation through grant MCB-0920261.

References

1. Ohtaki, H.; Radnai, T. *Chemical Reviews* **1993**, *93*, 1157–1204.
2. Roux, B.; Bernèche, S.; Egwolf, B.; Lev, B.; Noskov, S. Y.; Rowley, C. N.; Yu, H. *J. Gen. Physiol.* **2011**, *137*, 415–426.
3. Shannon, R. D. *Acta Cryst.* **1976**, *A32*, 751–767.
4. Marcus, Y. *Biophys. Chem.* **1994**, *51*, 111–127.
5. Piquemal, J.-P.; Perera, L.; Cisneros, G. A.; Ren, P.; Pedersen, L. G.; Darden, T. A. *J. Chem. Phys.* **2006**, *125*, 054511.
6. Wu, J. C.; Piquemal, J.-P.; Chaudret, R.; Reinhardt, P.; Ren, P. *J. Chem. Theory Comput.* **2010**, *6*, 2059–2070.
7. Yu, H.; Whitfield, T. W.; Harder, E.; Lamoureux, G.; Vorobyov, I.; Anisimov, V. M.; MacKerell, A. D.; Roux, B. *J. Chem. Theory Comput.* **2010**, *6*, 774–786.
8. Kulik, H. J.; Marzari, N.; Correa, A. A.; Prendergast, D.; Schwegler, E.; Galli, G. *J. Phys. Chem. B* **2010**, *114*, 9594–9601.
9. Lightstone, F. C.; Schwegler, E.; Hood, R. Q.; Gygi, F.; Galli, G. *Chem. Phys. Lett.* **2001**, *343*, 549 – 555.
10. Di Tommaso, D.; de Leeuw, N. H. *Crystal Growth & Design* **2010**, *10*, 4292–4302.
11. Bhattacharjee, A.; Pribil, A. B.; Randolf, B. R.; Rode, B. M.; Hofer, T. S. *Chem. Phys. Lett.* **2012**, *536*, 39–44.
12. Ikeda, T.; Boero, M.; Terakura, K. *J. Chem. Phys.* **2007**, *127*, 074503.
13. Cauet, E.; Bogatko, S.; Weare, J. H.; Fulton, J. L.; Schenter, G. K.; Bylaska, E. J. *J. Chem. Phys.* **2010**, *132*, 194502.
14. Fatmi, M. Q.; Hofer, T. S.; Randolf, B. R.; Rode, B. M. *J. Chem. Phys.* **2005**, *123*, 054514.
15. Rega, N.; Brancato, G.; Petrone, A.; Caruso, P.; Barone, V. *J. Chem. Phys.* **2011**, *134*, 074504.
16. Rowley, C. N.; Roux, B. *J. Chem. Theory Comput.* **2012**, *8*, 3526–3535.
17. Brooks, B. R. et al. *J. Comput. Chem* **2009**, *30*, 1545–1614.
18. *TURBOMOLE V6.3 2011, a development of University of Karlsruhe and Forschungszentrum Karlsruhe GmbH, 1989-2007, TURBOMOLE GmbH, since 2007; available from* `http://www.turbomole.com`.
19. Swope, W. C.; Andersen, H. C.; Berens, P. H.; Wilson, K. R. *J. Chem. Phys.* **1982**, *76*, 637–649.
20. van Gunsteren, W.; Berendsen, H. *Mol. Phys.* **1977**, *34*, 1311–1327.
21. Jorgensen, W. L.; Chandrasekhar, J.; Madura, J. D.; Impey, R. W.; Klein, M. L. *J. Chem. Phys.* **1983**, *79*, 926–935.
22. Lamoureux, G.; Harder, E.; Vorobyov, I. V.; Roux, B.; Jr., A. D. M. *Chem. Phys. Lett.* **2006**, *418*, 245–249.
23. Callahan, K. M.; Casillas-Ituarte, N. N.; Roeselova, M.; Allen, H. C.; Tobias, D. J. *J. Phys. Chem. A* **2010**, *114*, 5141–5148, PMID: 20201546.
24. Perdew, J. P.; Burke, K.; Ernzerhof, M. *Phys. Rev. Lett.* **1996**, *77*, 3865–3868.
25. Von Arnim, M.; Ahlrichs, R. *J. Comput. Chem* **1998**, *19*, 1746–1757.
26. Weigend, F. *Phys. Chem. Chem. Phys.* **2006**, *8*, 1057–1065.
27. Zhang, R.; Lev, B.; Cuervo, J. E.; Noskov, S. Y.; Salahub, D. R. In *Combining Quantum Mechanics and Molecular Mechanics. Some Recent Progresses in QM/MM Methods*; Sabin, J. R.; Brndas, E., Eds.; Academic Press, 2010, Vol. 59, pp 353–400.
28. Kumar, S.; Rosenberg, J. M.; Bouzida, D.; Swendsen, R. H.; Kollman, P. A. *J. Comput. Chem* **1992**, *13*, 1011–1021.
29. Lamoureux, G.; Roux, B. *J. Phys. Chem. B* **2006**, *110*, 3308–3322.
30. Hoover, W. G. *Phys. Rev. A* **1985**, *31*, 1695–1697.
31. Martyna, G. J.; Tobias, D. J.; Klein, M. L. *J. Chem. Phys.* **1994**, *101*, 4177–4189.
32. Deng, Y.; Roux, B. *The Journal of Physical Chemistry B* **2004**, *108*, 16567–16576.
33. Xiang, J. Y.; Ponder, J. W. *J. Comput. Chem* **2012**, n/a–n/a.
34. Bruni, F.; Imberti, S.; Mancinelli, R.; Ricci, M. A. *J. Chem. Phys.* **2012**, *136*, 064520.
35. D'Angelo, P.; Barone, V.; Chillemi, G.; Sanna, N.; Meyer-Klaucke, W.; Pavel, N. V. *Journal of the American Chemical Society* **2002**, *124*, 1958–1967, PMID: 11866609.

36. D'Angelo, P.; Benfatto, M.; Della Longa, S.; Pavel, N. V. *Phys. Rev. B* **2002**, *66*, 064209.

37. Roux, B.; Yu, H.; Karplus, M. *J. Phys. Chem.* **1990**, *94*, 4683–4–688.

38. Schmid, R.; Miah, A. M.; Sapunov, V. N. *Phys. Chem. Chem. Phys.* **2000**, *2*, 97–102.